INTERFACE

royalsocietypublishing.org/journal/rsif

Research

Cite this article: Nguyen MM, Freedman AS, Ozbay SA, Levin SA. 2023 Fundamental bound on epidemic overshoot in the SIR model. *J. R. Soc. Interface* **20**: 20230322. https://doi.org/10.1098/rsif.2023.0322

Received: 2 June 2023
Accepted: 6 November 2023

Subject Category:
Life Sciences–Mathematics interface

Subject Areas:
biomathematics, ecosystems, computational biology

Keywords:
epidemiology, SIR model, overshoot

Author for correspondence:
Maximilian M. Nguyen
e-mail: mmnguyen@princeton.edu

Electronic supplementary material is available online at https://doi.org/10.6084/m9.figshare.c.6935471.

THE ROYAL SOCIETY PUBLISHING

Fundamental bound on epidemic overshoot in the SIR model

Maximilian M. Nguyen[1], Ari S. Freedman[2], Sinan A. Ozbay[3] and Simon A. Levin[2]

[1]Lewis-Sigler Institute, [2]Department of Ecology and Evolutionary Biology, and [3]Bendheim Center for Finance, Princeton University, Princeton, NJ 08544, USA

MMN, 0000-0002-4378-5050; SAL, 0000-0002-8216-5639

We derive an exact upper bound on the epidemic overshoot for the Kermack–McKendrick SIR model. This maximal overshoot value of $0.2984\cdots$ occurs at $R_0^* = 2.151\cdots$. In considering the utility of the notion of overshoot, a rudimentary analysis of data from the first wave of the COVID-19 pandemic in Manaus, Brazil highlights the public health hazard posed by overshoot for epidemics with R_0 near 2. Using the general analysis framework presented within, we then consider more complex SIR models that incorporate vaccination.

1. Introduction

The overshoot of an epidemic is the proportion of the population that becomes infected after the peak of the epidemic has already passed. Formally, it is given as the difference between the fraction of the population that is susceptible at the peak of infection prevalence and at the end of the epidemic. Intuitively, it is the difference between the herd immunity threshold and the total fraction of the population that gets infected [1,2]. As it describes the damage to the population in the declining phase of the epidemic (i.e. when the effective reproduction number is less than 1), one might be tempted to dismiss its relative importance. However, a substantial proportion of the epidemic, and thus a large number of people, may be impacted during this phase of the epidemic dynamics.

A natural question to ask then is how large can the overshoot be and how does the overshoot depend on epidemic parameters, such as transmissibility and recovery rate? Surprisingly, this question can be answered exactly. In this paper, we first derive the bound on the overshoot in the Kermack–McKendrick limit of the SIR model [3]. We then compare the predictions of this feature of the SIR model with data taken from the first wave of the COVID-19 pandemic in Manaus, Brazil [4]. Beyond the basic SIR model, we then see if the bound on overshoot holds if we add additional complexity, such as vaccinations.

2. Results

Over the years, the Kermack–McKendrick SIR model has become largely synonymous with the following set of ordinary differential equations (ODEs) due to their simplicity and popularity:

$$\frac{dS}{dt} = -\beta SI, \tag{2.1}$$

$$\frac{dI}{dt} = \beta SI - \gamma I \tag{2.2}$$

and

$$\frac{dR}{dt} = \gamma I, \tag{2.3}$$

where S, I, and R are the fractions of population in the susceptible, infected, and recovered state, respectively. As these are the only possible states within

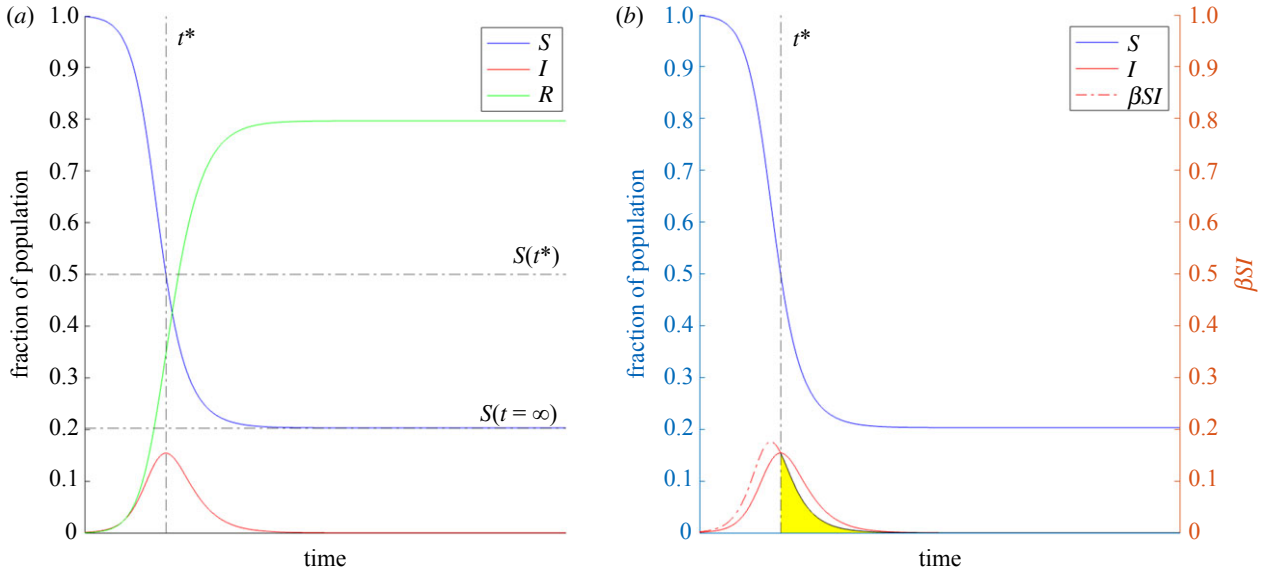

Figure 1. The overshoot can be calculated in two ways. (*a*) Overshoot is calculated as the difference between the fraction of the population that is susceptible at t^* and infinite time. (*b*) Overshoot is calculated as the integral of the infection incidence curve from t^* until infinite time. Therefore, overshoot corresponds to the area of the region shaded in yellow.

this model, the conservation equation for the whole population is given as $S+I+R=1$. It is worth noting that the original compartmental model formulated by Kermack and McKendrick in their seminal paper from a century ago [3] is actually a more general model than the ODE model that has become synonymous with their names. The original model considered both infectiousness that depended on the amount of time since becoming infected, which has been termed age-of-infection, and demographic effects in the form of deaths. A considerable amount has been learned and understood in the case of the more general model that considers age-of-infection (see [5,6] for an introduction), which typically takes the form of a nonlinear renewal equation. While here we have chosen to focus on the simpler ODE model, under certain assumptions our result for the overshoot can be carried over to the age-of-infection model as well.

Conceptually, the overshoot can be equivalently calculated in two ways. In the first, it is given by the difference in the fraction of susceptible individuals at the peak of infection prevalence (S_{t^*}) and at the end of the end of the epidemic (S_∞) (figure 1*a*). Alternatively, it can be viewed as the integration of the number of newly infected individuals, which is given by the infection incidence rate (βSI) from the peak of infection prevalence to the end of the epidemic (figure 1*b*). We will make use of the former relationship in the results that follow.

The only two parameters of the ODE model are β and γ. A key parameter in epidemic modelling combines these two into a single parameter by taking their ratio, which is known as the basic reproduction number (R_0). The behaviour of the overshoot can be shown to be only dependent on this single parameter, R_0. Plotting the dependency of overshoot on R_0 (figure 2), we observe a peak in the curve at (R_0^*, Overshoot*) that sets an upper bound on the overshoot. From a public health perspective, diseases that have estimated R_0 values near this peak region in figure 2 include COVID-19 (ancestral strain) [7], SARS [8], diphtheria [9], monkeypox [10], and ebola [11]. This peak phenomenon in the overshoot was first numerically observed by Zarnitsyna *et al.* [12], though not explained. We will now derive the solution for this maximum point analytically.

2.1. Deriving the exact bound on overshoot in the Kermack–McKendrick SIR model

Theorem 2.1. *The maximum possible overshoot in the Kermack–McKendrick SIR model is a fraction* $0.2984\cdots$ *of the entire population, with a corresponding* $R_0^* = 2.151\cdots$.

Proof. Let t^* be the time at the peak of the infection prevalence curve. Here, we define the herd immunity threshold as the difference in the fractions of the population that are susceptible at zero time and at t^*. Then, the overshoot is defined as the difference in the fractions of the population that are susceptible at t^* and at infinite time. This is equivalent to defining overshoot as the cumulative fraction of the population that gets infected after t^*.

$$\text{Overshoot} \equiv \int_{t^*}^{\infty} -\left(\frac{\mathrm{d}S}{\mathrm{d}t}\right)\mathrm{d}t = \int_{t*}^{\infty} \beta SI\,\mathrm{d}t = S_{t*} - S_\infty, \quad (2.4)$$

where S_{t^*} and S_∞ are the susceptible fractions at t^* and infinite time, respectively. We will use $S_{t^*} = 1/R_0$ [13], which can be obtained by setting (2.2) to zero and solving for that critical S. We will use the notation X_t to indicate the value of compartment X at time t.

$$\text{Overshoot} = \frac{1}{R_0} - S_\infty. \quad (2.5)$$

As an aside, it is worth noting that the result that follows also holds for the more general age-of-infection model [3] if we restrict our definition of the herd immunity threshold to be the fraction of people that need to be removed from the population at the beginning of the epidemic to prevent an outbreak from occurring. While this alternative definition gives an equivalent herd immunity threshold in the ODE model where it is defined in terms of the peak of the prevalence curve, this more robust definition is needed to account for the more complicated behaviour in the age-of-infection model.

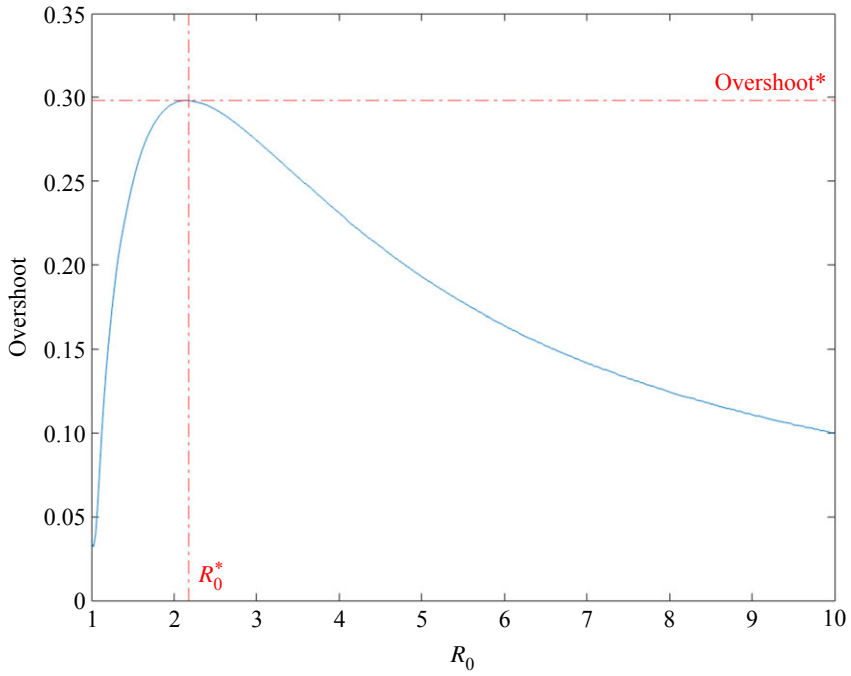

Figure 2. The overshoot as a function of R_0 for the Kermack–McKendrick SIR model.

Since we would like to compute maximal overshoot, we can differentiate the overshoot equation (2.5) with respect to S_∞ to find the extremum. We will eliminate R_0 from the overshoot equation so that we have an equation only in terms of S_∞.

To find an expression for R_0, we start by deriving the standard final size relation for the SIR model [14,15]. We solve for the rate of change of I as a function of S using (2.1) and (2.2) to obtain

$$\frac{\mathrm{d}I}{\mathrm{d}S} = -1 + \frac{\gamma}{\beta S},$$

from which it follows on integration that $S + I - (\gamma/\beta)\ln S$ is constant along any trajectory.

Considering the beginning of the epidemic and the peak of the epidemic yields

$$S_0 + I_0 - \frac{\gamma}{\beta}\ln S_0 = S_\infty + I_\infty - \frac{\gamma}{\beta}\ln S_\infty,$$

hence

$$\frac{\beta}{\gamma}(S_\infty - S_0 + I_\infty - I_0) = \ln\left(\frac{S_\infty}{S_0}\right). \tag{2.6}$$

We now define the initial conditions: $S_0 = 1 - \epsilon$ and $I_0 = \epsilon$, where ϵ is the (infinitesimally small) fraction of initially infected individuals. We assume that the number of initially infected individuals (ϵ) is much smaller than the size of the population (i.e. $\epsilon \ll 1$). For the scale that we have in mind, such as those of city populations and larger, it is thus reasonable to make the approximation $1 - \epsilon \approx 1$. We also use the standard asymptotic of the SIR model that there are no infected individuals at the end of an SIR epidemic: $I_\infty = 0$. Taking the above conditions together and recalling that $R_0 = \frac{\beta}{\gamma}$, we obtain that

$$S_\infty = \mathrm{e}^{R_0(S_\infty - 1)}. \tag{2.7}$$

The resulting equation (2.7) is the final size relation for the Kermack–McKendrick SIR model. Importantly, this final size relation taken together with the alternative definition for the herd immunity threshold implies the subsequent result for overshoot holds not only for the simpler ODE model considered here, but also for the more general age-of-infection model of Kermack & McKendrick [3]. The robustness of the final size relation in the context of the more general model can be more easily viewed through the lens of a renewal equation for the force of infection; see [6,15–17] for a derivation and a more complete discussion.

Rearranging for R_0 yields the following expression:

$$\frac{\ln(S_\infty)}{S_\infty - 1} = R_0. \tag{2.8}$$

We then substitute this R_0 expression (2.8) into the overshoot equation (2.5):

$$\text{Overshoot} = \frac{S_\infty - 1}{\ln(S_\infty)} - S_\infty. \tag{2.9}$$

Differentiating with respect to S_∞ and setting the equation to zero to find the maximum overshoot yields

$$(\ln S_{\infty *})^2 = \ln S_{\infty *} - 1 + \frac{1}{S_{\infty *}}, \tag{2.10}$$

whose solution is

$$S_{\infty *} = 0.1664\cdots,$$

and which corresponds to

$$\text{Overshoot}^* = 0.2984\cdots, \tag{2.11}$$

using (2.9). The corresponding R_0 calculated using (2.8) is

$$R_0^* = 2.151\cdots. \tag{2.12}$$

This concludes the proof. ∎

Additionally, to find the total recovered fraction is straightforward. In the asymptotic limit of the SIR model, there are no remaining infected individuals, so $R_{\infty *} = 1 - S_{\infty *}$:

$$R_{\infty *} = 1 - 0.1664\cdots = 0.8336\cdots. \tag{2.13}$$

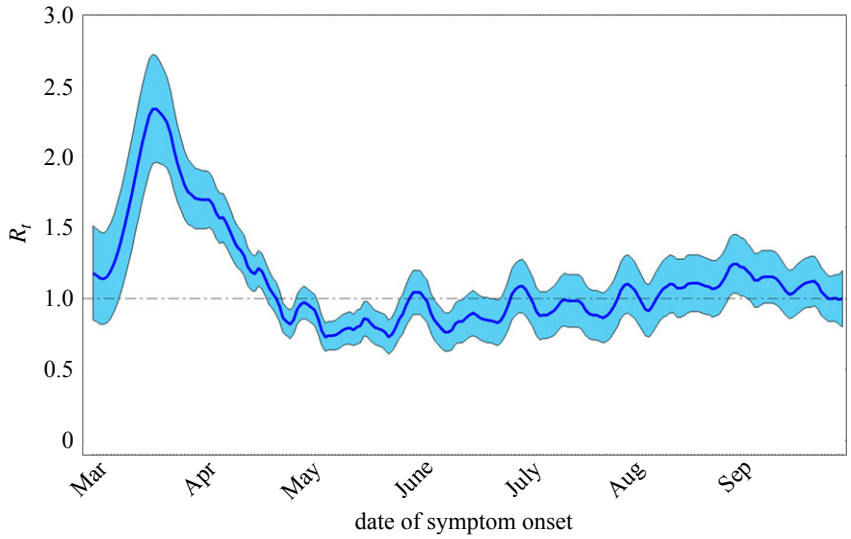

Figure 3. Effective reproduction number (R_t) in Manaus, Brazil in 2020 as a function of date of symptom onset. Light blue indicates 95% confidence interval around dark blue mean. Figure adapted from fig. S7.D in Buss *et al.* [4].

In other words, approximately 5 out of every 6 individuals in the population will have experienced infection when overshoot is maximized.

3. Conclusion

We have proved that the maximum fraction of the population that can be infected during the overshoot phase of an epidemic in the Kermack–McKendrick SIR model is just under 0.3, with a corresponding basic reproduction number of $R_0 \approx 2.15$.

Given the clear predictions of this feature of the SIR model, it is reasonable to ask whether the theory matches any real-world epidemics. While high-quality data on large, unmitigated epidemics (for which the SIR model would most directly apply) in human populations are rare, we will now perform a rudimentary analysis of data from the first wave of the COVID-19 pandemic in Manaus, Brazil as given by Buss *et al.* [4]. While the city did implement some small level of non-pharmaceutical interventions, for the purpose of calculation let us take at face value that the epidemic spread through the city practically unmitigated.

To estimate the theoretical prediction of overshoot in the SIR model, we need to first estimate R_0. The conservative, forward-looking approach we take here is to take the maximum of the effective reproduction number (R_t) when the epidemic is first starting. Using data from Buss *et al.* [4] for R_t in Manaus as a function of date of symptom onset, which we take as a proxy for time, the R_0 was approximately 2.3 in Manaus in mid-March (figure 3). For $R_0 = 2.3$, using figure 2 as a reference, the theoretical prediction for overshoot is approximately 29%. Thus, if R_0 can be estimated early on in the epidemic, the overshoot can be subsequently predicted within the context of an SIR model before the peak of the epidemic occurs, which in practice provides more time for public health measures and interventions to be implemented before the overshoot phase takes place.

To calculate the overshoot as observed directly from the data, we again refer to the time series data for R_t (figure 3). We will consider the time when $R_t = 1$ to be when the epidemic peaks (t^*). Reading the data suggests the first COVID-19 wave peaked in late April. We note that R_t stays around 1 until mid-August, when it starts rising again. As the basic SIR model does not consider such complex late-time behaviour, for the purpose of this analysis, we will consider the first wave to have ended by mid-August. We note that assigning an endpoint to the data is a strong assumption, and that actually determining the turning and end point of an epidemic in the context of epidemic forecasting is not a simple matter [18].

With the date of an epidemic peak in hand, we now turn to reading the prevalence curve. Specifically, we will be using the mean data given by seroreversion-adjusted prevalence at a 1.4 S/C threshold for positive detection (figure 4), which is adapted from Buss *et al.* [4]. The seroreversion adjustment is their best attempt for controlling for antibody waning. Given this correction, we will take this curve as the cumulative outbreak size. The 1.4 S/C threshold is based on the sampling threshold in relative light units for deciding whether a sample has a significant positive chemiluminescence signal over the calibration. After fitting the time series points to a simple logistic curve, it can be seen that when R_t first reached 1 (indicating the epidemic had peaked), the cumulative fraction of the population that had been infected was approximately 36%. From here, we see that the cumulative fraction that becomes infected between this time point when R_t first reached 1 and the end of the first wave in mid-August (i.e. the overshoot) is 30% from the data.

We, therefore, see that the SIR model prediction for overshoot aligns with the value derived from the data, suggesting that the dynamics of the first wave of COVID-19 in Manaus, Brazil can be approximated by a simple SIR model. While the crude analysis above makes several strong assumptions about the nature of the unmitigated spread, the endpoint of the wave, the accuracy of the seroprevalence testing and correction methods, and the fidelity of the sampling intervals, the fit between the data and a SIR model is perhaps unsurprising given the relatively high population density of Manaus and general lack of thorough mitigation measures. To a first-order approximation, the data suggest that overshoot indeed poses a significant amount of public

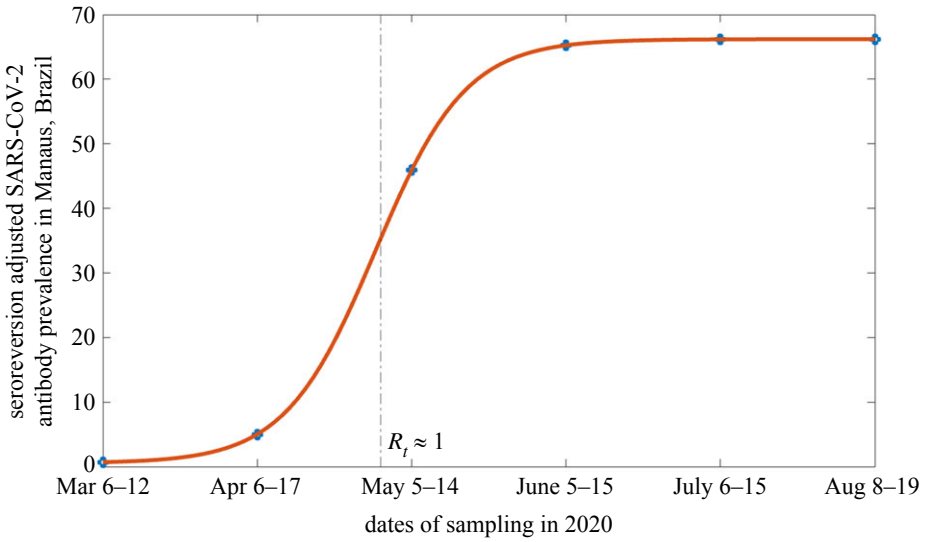

Figure 4. Mean cumulative antibody prevalence in Manaus, Brazil in 2020. Seroreversion adjustment done with a 1.4 S/C threshold. Figure adapted from the red points in fig. 2A and table S2 in Buss *et al.* [4].

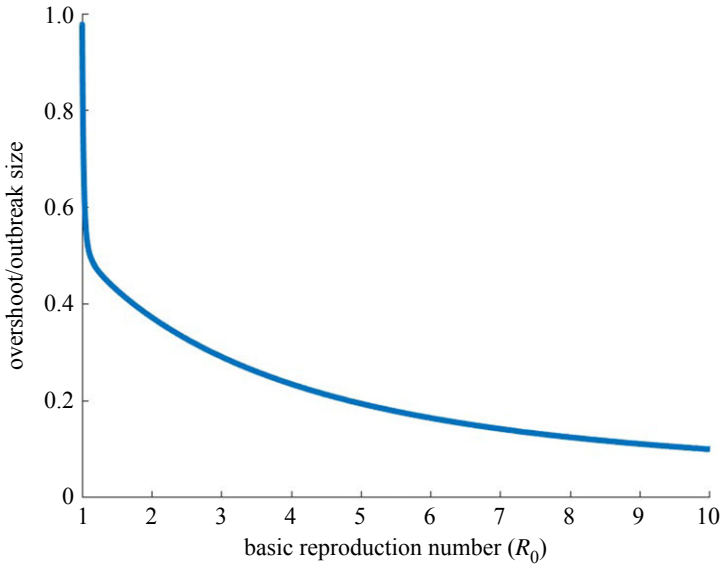

Figure 5. The ratio of individuals infected in the overshoot phase compared to total outbreak size as a function of R_0.

health hazard when R_0 is in the neighbourhood of 2. And that for well-mixed, unmitigated epidemics that may be approximated by SIR dynamics, overshoot may be a sizeable portion of the dynamics and overall attack rate.

The mathematical intuition on why there is a peak in the overshoot as a function of R_0 can be seen by inspection of equation (2.5). The first term, $1/R_0$, monotonically decreases with increasing R_0. The last term, $-S_\infty$, monotonically increases with R_0. Thus a trade-off in the two terms results in a single intermediate peak. The epidemiological intuition behind a peak in the overshoot is that the total number of individuals infected during the epidemic grows monotonically with increasing R_0. However, too high of an R_0 leads to a sharp growth in the number of infected individuals, which burns through most of the population before the infection prevalence peak is reached, leaving few susceptible individuals left for the overshoot phase. This is seen by a monotonic decrease in the fraction of infected individuals that occurs in the overshoot phase with increased R_0 (figure 5). Thus the maximal overshoot occurs as a trade-off between those two directions. It is interesting to note that while the overshoot is a non-monotonic function of R_0, in contrast, the ratio of overshoot to outbreak size is a strictly decreasing function of R_0 (see appendix A for further discussion).

The fundamental upper bound on the overshoot derived here also seems to hold under the addition of more complexity into the SIR model (see appendix A). Upon the addition of different modes of vaccination, we find the bound on overshoot still holds in all cases considered. In the 2-strain with vaccination SIR model of Zarnitsyna *et al.* [12], the overshoot depends on both the level of strain dominance and vaccination rate, but from their results it is numerically seen that any amount of vaccination will produce an overshoot lower than the bound found here. Different control measures and strategies may reduce the overshoot as compared to the unmitigated case [1], keeping this upper bound intact. Future work may explore how general this bound is for SIR models with other types of complexities or for models beyond the SIR type.

Ethics. This work did not require ethical approval from a human subject or animal welfare committee.

Data accessibility. Supplementary material is available online [19].

Declaration of AI use. We have not used AI-assisted technologies in creating this article.

Authors' contributions. M.M.N.: conceptualization, formal analysis, investigation, methodology, supervision, visualization, writing—original draft, writing—review and editing; A.S.F.: formal analysis, investigation, methodology, writing—original draft, writing—review and editing; S.A.O.: formal analysis, investigation, methodology, visualization, writing—original draft, writing—review and editing; S.A.L.: formal analysis, funding acquisition, investigation, methodology, writing—original draft, writing—review and editing.

All authors gave final approval for publication and agreed to be held accountable for the work performed therein.

Conflict of interest declaration. We declare we have no competing interests.

Funding. The authors would like to acknowledge generous funding support provided by the National Science Foundation (grant nos. CCF1917819 and CNS-2041952), the Army Research Office (grant no. W911NF-18-1-0325) and a gift from the William H. Miller III 2018 Trust.

Acknowledgements. The authors would like to acknowledge Bryan Grenfell and Chadi Saad-Roy for their useful suggestions.

Appendix A

A.1. Upper bounds on overshoot in models that include vaccinations

Beyond the Kermack–McKendrick SIR model, one can ask if the bound on overshoot still holds if other complexities are added to the model. First, we will consider the addition of vaccinations.

We will consider three qualitatively different types of curves for the vaccination rate (figure 6). These correspond to different scenarios that might be modelled. The first model assumes a vaccination rate of zero after the outbreak begins, which implies all vaccinations occur before the outbreak. The second model of vaccination assumes a constant *per capita* vaccination rate. This is a situation where all susceptible individuals get vaccinated at the same rate. This assumption yields a vaccination curve for the population that is concave down. The third type of model assumes a risk-driven vaccination rate that depends on the number of infected individuals. This yields a non-monotonic vaccination curve for the population that switches from being initially concave up to being concave down. Depending on the scenario being analysed, one model might be more appropriate to use than others. Below we discuss each model in further detail by providing the corresponding system of equations, relevant scenarios the model might correspond to in reality, and the corresponding maximal overshoot for each model.

A.1.1. Maximal overshoot when the number of vaccinated individuals is constant

The first model of vaccination assumes there are no vaccinations during the outbreak, which implies a fixed number of vaccinated individuals over the course of the epidemic. Such a scenario might be the reintroduction of an infectious disease into a population that has a pre-existing level of immunity.

Since the number of vaccinated individuals is constant, this implies all vaccinations occurred prior to the initial time step. The calculation is then trivial assuming

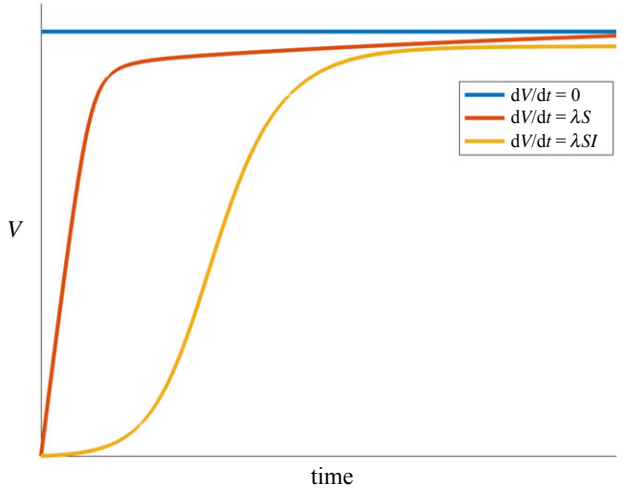

Figure 6. The fraction of population that is vaccinated (V) based on different vaccination rates: a vaccination rate of zero over the course of the epidemic (blue), a constant *per capita* vaccination rate (orange), and a risk-driven vaccination rate (yellow).

vaccinations provide complete and permanent immunity. In that case, vaccinated individuals can simply be ignored entirely in the dynamics, resulting in the maximal overshoot simply scaling with the unvaccinated fraction.

$$\text{Overshoot}^*_{\text{SIRV}} = (1 - V)0.2984\cdots. \tag{A 1}$$

A.1.2. Maximal overshoot under addition of constant *per capita* vaccination

We next consider a more typical scenario where the vaccination rate per unvaccinated individual is constant per unit time. Barring any additional information about the population or the epidemic, it is reasonable to assume that all susceptible individuals are vaccinated at the same rate. Consider the following SIRV model:

$$\frac{\mathrm{d}S}{\mathrm{d}t} = -\beta SI - \lambda S, \tag{A 2}$$

$$\frac{\mathrm{d}I}{\mathrm{d}t} = \beta SI - \gamma I, \tag{A 3}$$

$$\frac{\mathrm{d}R}{\mathrm{d}t} = \gamma I \tag{A 4}$$

and

$$\frac{\mathrm{d}V}{\mathrm{d}t} = \lambda S. \tag{A 5}$$

In this case, it is easily shown that there is a conserved quantity, $S + I - (\gamma/\beta)\ln S + (\lambda/\beta)\ln I$, which reduces to (2.6) when the vaccination rate is zero (i.e. $\lambda = 0$). Unfortunately, having the conserved quantity is not sufficient to compute the overshoot, since there does not appear to be a way to separate infected and vaccinated individuals when trying to extend the previous calculation. Therefore, we turn to numerical computation (figure 7*a*). We find that the maximal overshoot is bounded above by the value already obtained in the model without vaccinations. As shown in figure 7*b*, the overshoot has a complicated dependence on the vaccination parameter λ and R_0.

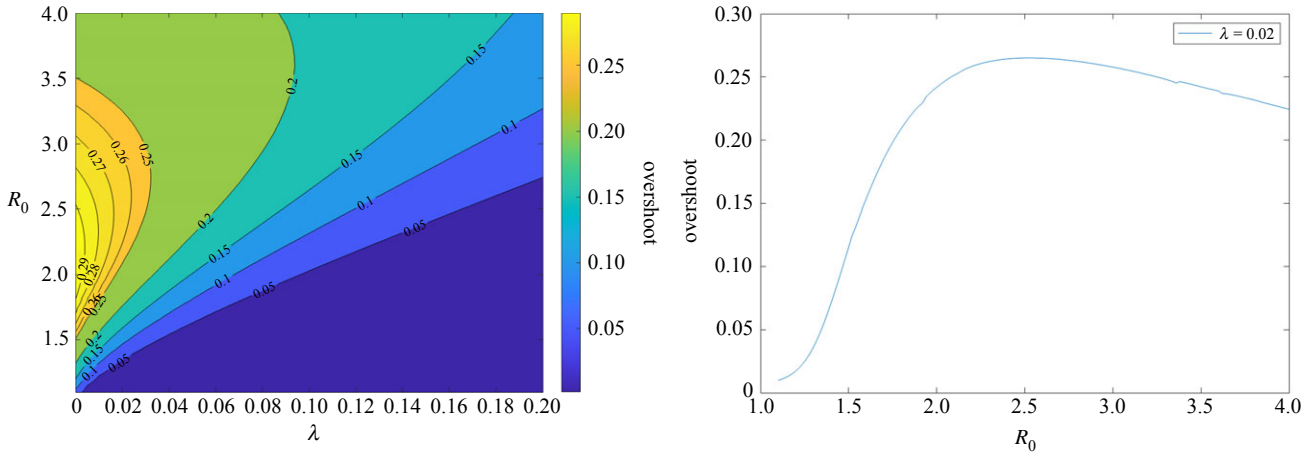

Figure 7. (*a*) Contour plot for the overshoot for the SIRV model with $dV/dt = \lambda S$ as a function of λ and R_0. (*b*) Vertical cross-section of the contour plot from (*a*) for $\lambda = 0.02$.

A.1.3. Maximal overshoot under addition of a risk-driven vaccination rate

Lastly consider a vaccination rate that is proportional to the number of infected individuals. Such risk-driven behaviour may arise for a variety of reasons, including initial vaccine hesitancy, a delay in vaccine availability, or a correlation between willingness to get vaccinated and the number of infected individuals. Consider the following SIRV model:

$$\frac{dS}{dt} = -\beta SI - \lambda SI, \tag{A 6}$$

$$\frac{dI}{dt} = \beta SI - \gamma I, \tag{A 7}$$

$$\frac{dR}{dt} = \gamma I \tag{A 8}$$

and

$$\frac{dV}{dt} = \lambda SI. \tag{A 9}$$

Since the model now has an additional compartment, V, compared with the original SIR model, we must update our definition for overshoot accordingly. Fundamentally, overshoot compares the fraction of people who have not been infected at the epidemic peak and the people who have not been infected at the end of the epidemic. The fraction of people who have not been infected at any particular time, t, is $S_t + V_t$. Thus, overshoot can be redefined as follows:

$$\text{Overshoot} = (S_{t^*} + V_{t^*}) - (S_\infty + V_\infty).$$

Since the equation for dI/dt remains unchanged, $S_{t^*} = 1/R_0$ still applies. Thus, the overshoot equation for models with vaccinated compartments is given by

$$\text{Overshoot} = \left(\frac{1}{R_0} + V_{t^*}\right) - (S_\infty + V_\infty). \tag{A 10}$$

To maximize overshoot, we thus need to find expressions for R_0, V_{t^*} and V_∞ in terms of S_∞.

To find R_0, we start by taking the ratio dI/dS and integrating as before. It follows that $I + (\beta/(\beta+\lambda))S - (\gamma/(\beta+\lambda))\ln S$ is constant along any trajectory. Considering the beginning and the end of the epidemic yields

$$I_0 + \frac{\beta}{\beta+\lambda}S_0 - \frac{\gamma}{\beta+\lambda}\ln S_0 = I_\infty + \frac{\beta}{\beta+\lambda}S_\infty - \frac{\gamma}{\beta+\lambda}\ln S_\infty.$$

Using the same initial conditions, asymptotic behaviour, and parameter substitution as before ($S_0 = 1-\epsilon$, $I_0 = \epsilon$, $I_\infty = 0$, $R_0 = \beta/\gamma$) yields the following final size relation:

$$R_0 = \frac{\ln(S_\infty)}{S_\infty - 1}. \tag{A 11}$$

Thus, we see that R_0 for this SIRV model takes on the same expression as that for the SIR model (2.8).

To find V_{t^*}, let us take the ratio of time derivatives of the S and V compartments (A 6) and (A 9):

$$\frac{(dS/dt)}{dV/dt} = \frac{-\beta SI - \lambda SI}{\lambda SI}$$

and

$$\frac{dS}{dV} = -\left(\frac{\beta+\lambda}{\lambda}\right),$$

from which it follows on integration that $S + ((\beta+\lambda)/\lambda)V$ is constant along any trajectory. Considering the beginning and the peak of the epidemic yields

$$S_0 + \left(\frac{\beta+\lambda}{\lambda}\right)V_0 = S_{t^*} + \left(\frac{\beta+\lambda}{\lambda}\right)V_{t^*}.$$

Using the initial conditions ($S_0 = 1-\epsilon$, $I_0 = \epsilon$, $V_0 = 0$) and recalling that $S_{t^*} = 1/R_0$, we obtain the following formula for V_{t^*}:

$$V_{t^*} = \left(1 - \frac{1}{R_0}\right)\left(\frac{\lambda}{\beta+\lambda}\right). \tag{A 12}$$

To find V_∞, recall that $S + ((\beta+\lambda)/\lambda)V$ is constant along any trajectory. Considering the peak of the epidemic and the end of the epidemic yields

$$S_{t^*} + \left(\frac{\beta+\lambda}{\lambda}\right)V_{t^*} = S_\infty + \left(\frac{\beta+\lambda}{\lambda}\right)V_\infty.$$

Using the equation for V_{t^*} (A 12) and recalling that $S_{t^*} = 1/R_0$, we obtain the following equation for V_∞:

$$V_\infty = (1 - S_\infty)\left(\frac{\lambda}{\beta+\lambda}\right). \tag{A 13}$$

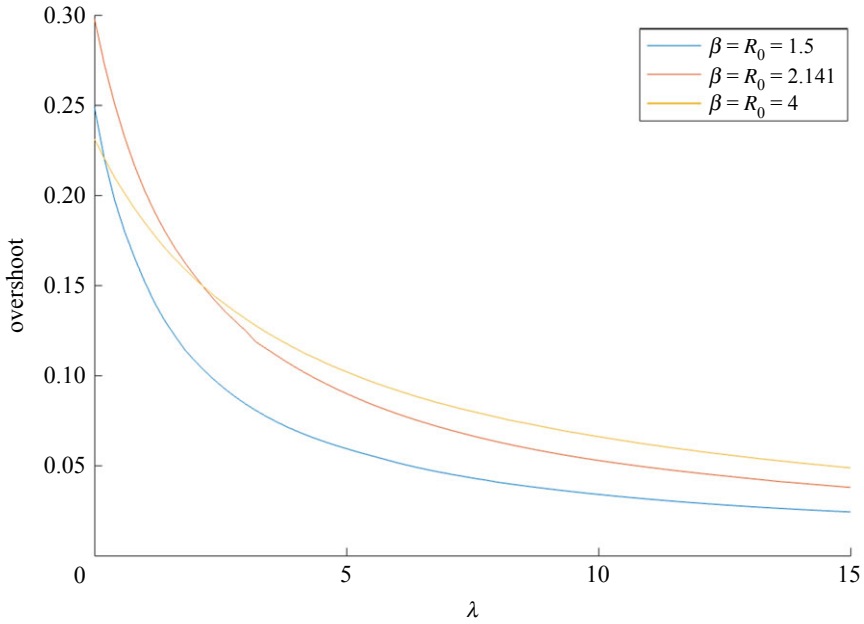

Figure 8. The overshoot for the SIRV model with $dV/dt = \lambda SI$ as a function of λ for different levels of β (or equivalently R_0).

Substituting the expressions for R_0 (A 11), V_{t^*} (A 12), V_∞ (A 13) into the overshoot equation (A 10) yields

$$\text{Overshoot} = \left(\frac{S_\infty - 1}{\ln(S_\infty)} - S_\infty\right)\left(1 - \frac{\lambda}{\beta + \lambda}\right). \tag{A 14}$$

We see that this expression for the overshoot is simply the overshoot expression for the original SIR model (2.9) scaled by a factor $1 - (\lambda/(\beta + \lambda))$:

$$\text{Overshoot}_{\text{SIRV}(\lambda SI)} = \text{Overshoot}_{\text{SIR}}\left(1 - \frac{\lambda}{\beta + \lambda}\right). \tag{A 15}$$

Assuming $\beta > 0$, $\lambda \geq 0$, then the factor $1 - (\lambda/(\beta + \lambda))$ can never be greater than 1. This implies that the bound on maximal overshoot given by the theorem holds, becoming exact in the limit of no vaccinations (i.e. $\lambda = 0$). For this model, the maximal overshoot decreases as a function of λ in a nonlinear way and has a nonlinear dependence on R_0 (figure 8).

A.2. The ratio of overshoot to outbreak size

In the main text, we consider the calculation of overshoot alone. It is also interesting to ask how the overshoot compares to the final attack rate given by the outbreak size. It turns out we can do the calculation analytically using the previous definition for Overshoot $= (1/R_0) - S_\infty$ (equation (2.5)) and defining the total outbreak size as Outbreak Size $= 1 - S_\infty = R_\infty$.

Taking the ratio of the two definitions yields

$$\frac{\text{Overshoot}}{\text{Outbreak Size}} = \frac{(1/R_0) - S_\infty}{1 - S_\infty} = \frac{1}{R_0(1 - S_\infty)} - \frac{S_\infty}{1 - S_\infty}. \tag{A 16}$$

Substituting R_0 using the relationship given by (2.8) yields

$$\frac{\text{Overshoot}}{\text{Outbreak Size}} = \frac{-1}{\ln S_\infty} - \frac{S_\infty}{1 - S_\infty}. \tag{A 17}$$

Differentiating this equation with respect to S_∞ and setting it to zero to find the extremal points S_∞^* yields

$$\frac{d(\text{Overshoot}/\text{Outbreak Size})}{dS_\infty} = 0 = \frac{1}{S_\infty^*(\ln S_\infty^*)^2} - \frac{1}{(1 - S_\infty^*)^2}. \tag{A 18}$$

It can be seen upon inspection that the only real solution for $(1 - S_\infty^*)^2 = S_\infty^*(\ln S_\infty^*)^2$ is at the point $S_\infty^* = 1$. This only occurs in the limit of $R_0 = 1$. Thus, at $R_0 = 1$, the overshoot exactly equals the outbreak size. Then, the overshoot becomes a strictly decreasing fraction of the total outbreak size with increasing R_0.

It can be shown that the only real solution to $(1 - S_\infty^*)^2 = S_\infty^*(\ln S_\infty^*)^2$ for $0 \leq S_\infty^* \leq 1$ is at the point $S_\infty^* = 1$.

Since $S_\infty^* = 0$ is clearly not a solution, we rule that out. Since $(1 - S_\infty^*)^2 = S_\infty^*(\ln S_\infty^*)^2$ at $S_\infty^* = 1$, it suffices to show that $f(S_\infty^*) := (1 - S_\infty^*)^2 - S_\infty^*(\ln S_\infty^*)^2 > 0$ for all $0 < S_\infty^* < 1$. Since $f'(S_\infty^* = 1) = 0$, it suffices to show that $f''(S_\infty^*) = (2(S_\infty^* - 1 - \ln S_\infty^*))/S_\infty^* > 0$ for all $0 < S_\infty^* < 1$. Since $\ln x < x - 1$ for all $x \neq 1$, then it follows that the second derivative must be positive.

References

1. Handel A, Longini IM, Antia R. 2007 What is the best control strategy for multiple infectious disease outbreaks? *Proc. R. Soc. B* **274**, 833–837. (doi:10.1098/rspb.2006.0015)
2. Cobey S. 2020 Modeling infectious disease dynamics. *Science* **368**, 713–714. (doi:10.1126/science.abb5659)
3. Kermack WO, McKendrick AG, Walker GT. 1927 A contribution to the mathematical theory of epidemics. *Proc. R. Soc. Lond. A* **115**, 700–721. (doi:10.1098/rspa.1927.0118)
4. Buss LF *et al.* 2021 Three-quarters attack rate of SARS-CoV-2 in the Brazilian Amazon during a largely unmitigated epidemic. *Science* **371**, 288–292. (doi:10.1126/science.abe9728)
5. Brauer F. 2005 The Kermack–McKendrick epidemic model revisited. *Math. Biosci.* **198**, 119–131. (doi:10.1016/j.mbs.2005.07.006)

6. Breda D, Diekmann O, de Graaf WF, Pugliese A, Vermiglio R. 2012 On the formulation of epidemic models (an appraisal of Kermack and McKendrick). *J. Biol. Dyn.* **6**, 103–117. (doi:10.1080/17513758.2012.716454)
7. Billah MA, Miah MM, Khan MN. 2020 Reproductive number of coronavirus: a systematic review and meta-analysis based on global level evidence. *PLoS ONE* **15**, e0242128. (doi:10.1371/journal.pone.0242128)
8. World Health Organization. 2003 *Consensus document on the epidemiology of severe acute respiratory syndrome (SARS)*. Geneva, Switzerland: WHO.
9. Truelove SA, Keegan LT, Moss WJ, Chaisson LH, Macher E, Azman AS, Lessler J. 2020 Clinical and epidemiological aspects of diphtheria: a systematic review and pooled analysis. *Clin. Infect. Dis.* **71**, 89–97. (doi:10.1093/cid/ciz808)
10. Grant R, Nguyen LBL, Breban R. 2020 Modelling human-to-human transmission of monkeypox. *Bull. World Health Organ.* **98**, 638–640. (doi:10.2471/BLT.19.242347)
11. Wong ZSY, Bui CM, Chughtai AA, Macintyre CR. 2017 A systematic review of early modelling studies of Ebola virus disease in West Africa. *Epidemiol. Infect.* **145**, 1069–1094. (doi:10.1017/S0950268817000164)
12. Zarnitsyna VI, Bulusheva I, Handel A, Longini IM, Halloran ME, Antia R. 2018 Intermediate levels of vaccination coverage may minimize seasonal influenza outbreaks. *PLoS ONE* **13**, e0199674. (doi:10.1371/journal.pone.0199674)
13. May RM. 1982 Vaccination programmes and herd immunity. *Nature* **300**, 481–483. (doi:10.1038/300481a0)
14. Arino J, Brauer F, Watmough J, Wu J. 2007 A final size relation for epidemic models. *Math. Biosci. Eng.* **4**, 159. (doi:10.3934/mbe.2007.4.159)
15. Brauer F. 2008 Age-of-infection and the final size relation. *Math. Biosci. Eng.* **5**, 681. (doi:10.3934/mbe.2008.5.681)
16. Thieme HR. 2018 *Mathematics in population biology*. Princeton, NJ: Princeton University Press.
17. Diekmann O, Heesterbeek H, Britton T. 2013 *Mathematical tools for understanding infectious disease dynamics*. Princeton, NJ: Princeton University Press.
18. Castro M, Ares S, Cuesta JA, Manrubia S. 2020 The turning point and end of an expanding epidemic cannot be precisely forecast. *Proc. Natl Acad. Sci. USA* **117**, 26 190–26 196. (doi:10.1073/pnas.2007868117)
19. Nguyen MM, Freedman AS, Ozbay SA, Levin SA. 2023 Fundamental bound on epidemic overshoot in the SIR model. Figshare. (doi:10.6084/m9.figshare.c.6935471)